

Kinetics of director gliding on a polymer–liquid-crystal interface

I. Jánošy

Research Institute for Solid State Physics and Optics, Hungarian Academy of Sciences, P.O. Box 49, H-1525 Budapest, Hungary

(Received 13 October 2009; published 30 March 2010)

Magnetic-field-induced surface reorientation of nematic liquid crystals on polyethyl-methacrylate films is studied. The experiments indicate that the time scale of director gliding expands from a fraction of a second to several hours. A power-law distribution function of relaxation times provides very good agreement between measurements and calculated gliding curves. From the model an upper limit of the extrapolation length can be extracted, which points to a surprisingly strong equilibrium azimuthal anchoring of the liquid crystal on the polymer layer.

DOI: [10.1103/PhysRevE.81.031714](https://doi.org/10.1103/PhysRevE.81.031714)

PACS number(s): 61.30.Hn, 68.08.—p

I. INTRODUCTION

The alignment properties of liquid crystals on solid substrates have been studied over decades and continue to be an active field of research even recently. The investigations are very important because the response of nematic liquid crystal layers to electric, magnetic and optical fields depends crucially on the boundary conditions at the liquid-crystal substrate interface. In the limiting case of “strong anchoring” the director alignment can be considered to be fixed at the cell boundaries; it is not influenced by the external field-induced deformation of the liquid crystal. In a more refined approximation the substrate can be characterized by an “easy axis,” i.e., the axis along which the interaction energy between the substrate and the liquid crystal is minimal [1]. The deviation of the director alignment from the easy axis gives rise to a surface torque (characterized by the anchoring energy or the extrapolation length [1]), which is balanced by the elastic torque of the liquid crystal at the interface. The balance of surface torques is established in microseconds [2], therefore, in a typical experiment it can be supposed to hold instantaneously.

As first demonstrated by Vetter *et al.* [3] and Vorflusev *et al.* [4] on polyvinyl alcohol (PVA) coatings, in certain cases a continuous realignment of the surface director is observed on a time scale much longer than the characteristic time for bulk distortions of the liquid crystalline film (director gliding). Several papers were published in connection with this phenomenon [5–9].

It is usually assumed that director gliding is connected with the reorientation of the easy axis under the influence of director deformation. Two mechanisms were proposed to be responsible for the realignment of the easy axis. In the first model, it was suggested that the easy axis is determined by the orientation of the liquid crystal molecules adsorbed at the substrate. When a director gradient is created at the interface along the normal direction to the plane, the adsorbed molecules change their orientation through desorption and readorption processes; in this way the easy axis rotates toward the surface director. The second mechanism is specific for polymers and azimuthal gliding. Its starting point is the assumption that under the influence of the anisotropic field of the liquid crystal the structure of the polymer network may be modified [8]. According to this model, the easy axis is

determined by the orientational distribution of the polymer chain segments. If the easy axis is not parallel to the surface director, conformational transitions occur in the polymer chains, again in a way to shift the easy axis toward the director. The latter model is supported by the fact that the drift of the easy axis speeds up by orders of magnitudes when the temperature range of glasslike to rubberlike behavior of the polymer is approached. We note that both mechanisms can lead also to the change of the anchoring energy at the interface that can have a contribution to the gliding process.

In this paper, we investigate the kinetics of magnetic-field-induced azimuthal gliding of a nematic liquid crystal on a polymer layer. The polymer used in the experiments was poly-ethyl-methacrylate (PEMA). The measurements were carried out with a setup containing a photoelastic modulator [10]. As discussed in Sec. II., the setup allows for the simultaneous determination of the director alignment and twist deformation at the interface. Two types of measurements were carried out. In the first kind of experiment the director alignment at the interface (i.e., the gliding angle) was kept fixed by continuously adjusting the magnetic field; meanwhile the variation of the surface twist deformation was detected. The advantage of this measurement technique over the one with fixed magnetic field is that the gliding angle is limited to relatively small values and its interpretation is more straightforward. From such measurements the long-term behavior of gliding could be followed. The second type of experiment was designed to probe the realignment of the surface director on short time scales. The magnetic field was applied only for an interval of the order of a second; the transient behavior of the orientation of the surface director and the twist deformation was registered on an oscilloscope. In the latter experiments the bulk elastic director equilibrium was not established during the measurement time, therefore the traditional criteria of gliding, i.e., that it occurs on long time scales, cannot be applied. To decide whether the change of surface director was due to elastic anchoring or gliding, we plotted the surface director angle against the surface twist. In the case of pure elastic anchoring this curve should be a straight line, the slope of which yields the extrapolation length [10]. In fact, the curves deviated considerably from a linear curve; moreover significant hysteresis was observed for up and down variation of the gliding angle, even with the shortest application period of the magnetic field (0.5 s). This circumstance indicates that the easy axis or/and the anchor-

ing strength must have changed during the application of the magnetic field, which we consider as a sign of gliding. The experimental findings are presented in Sec. III.

The interpretation of the results is given in Sec. IV. We use the model based on the rearrangement of polymer chains under the influence of the molecular field of the liquid crystal [8]. In the model a wide distribution of relaxation times is assumed for the gliding process. The distribution function can be only determined from the experiments. It was found that both the long and short time experiments can be very well described by a power-law distribution of the relaxation times, with a cut-off time at short times. With this form of the distribution function there are three parameters entering in the model, the initial elastic anchoring energy (or extrapolation length), the cutoff time and the exponent of the distribution function. The first two parameters, however, could not be independently determined from the measurements. An excellent fit was achieved with a wide range of cutoff times choosing appropriately the initial extrapolation length. As it is pointed out in the paper, this fact indicates that the cut-off relaxation time is much shorter than the time scale on which significant changes of the gliding angle occurs. The part of the distribution function with relaxation times shorter than the time interval on which noticeable gliding occurs can be included into the elastic contribution of the surface director reorientation. As a consequence the elastic process and gliding are indistinguishable. Nevertheless, from the short-time measurements an upper limit of the cutoff time could be obtained, which was found to be in the present experiments in the order of 0.1 s. From this fact we conclude that gliding is important already in time intervals as short as a fraction of a second or even shorter. A similar upper limit was established for the extrapolation length, which turned out to be in the order of a few nanometers. Consequently, according to our model, the azimuthal anchoring of the liquid crystal on poly-ethyl-methacrylate is very strong; it is comparable with that on rubbed poly-imide [11]. It was found furthermore that the exponent belonging to the long-term asymptotic distribution is about twice of the exponent belonging to the short-time distribution. A possible reason for this fact is suggested in the paper.

II. EXPERIMENTAL

The sample was similar to the one used in our previous experiments [8]. A nematic liquid crystal was sandwiched between two glass plates. One substrate was coated with a unidirectionally rubbed poly-imide layer, which ensured strong anchoring of the director on it. The other plate was coated with PEMA without any mechanical treatment. The cell thickness was 74.4 μm . The nematic liquid crystal was the eutectic mixture E63 from British Drog House (BDH), doped with a small amount of chiral dopant (C15 from BDH). After filling the cell and heating it above the glass transition temperature of PEMA (56 $^{\circ}\text{C}$), a twisted planar director configuration was obtained (due to chiralization) with a twist angle of 62 $^{\circ}$.

The experimental setup was the similar to the one used in [10]. A white light source was used, rather than a laser, in

order to avoid interference effects. The light was polarized parallel to the rubbing direction. It entered the sample from the polyimide side; behind the cell it passed through a photoelastic modulator (PEM) and an analyzer. The analyzer was attached to the PEM and was set 45 $^{\circ}$ with respect to its principal axis. The first and second harmonic components of the light signal were detected with two lock-in amplifiers. The sample was placed into an electromagnet with the rubbing direction parallel to the magnetic field. The magnetic field was controlled through a computer, which also collected the data from the lock-in amplifiers. The sample temperature was regulated with a thermostat with a precision of 0.1 $^{\circ}$.

As discussed in detail in [10], the strength of the second harmonic signal (SHS), I_2 , is related to the angle between the director at the exit face of the cell and the principal axis of the PEM, φ_L ,

$$I_2 = a \sin 2\varphi_L, \quad (1)$$

where a is a constant, depending on the refractive indices of the liquid crystal, the spectral distribution of the light source, the spectral sensitivity of the detector and the amplitude of the vibration of the quartz plate of the PEM. The quantity a was calibrated by rotating the PEM together with the analyzer by 4 $^{\circ}$ without applying magnetic field and detecting the change in I_2 . The strength of the first harmonic signal (FHS), I_1 , is related to the twist deformation at the exit interface, $d\varphi/dz|_{z=L} = \theta_L$, where z is the axis normal to the cell substrates,

$$I_1 = b\theta_L. \quad (2)$$

The constant b depends on the same parameters as a . It was calibrated from the value of I_1 before applying magnetic field; in this case $\theta_L = \theta_0 = \varphi_t/L$, where φ_t denotes the twist angle of the cell (62 $^{\circ}$) and L denotes the thickness of the liquid crystal layer.

III. MEASUREMENTS

A. Long-term measurements

In this type of measurements, we kept the gliding angle fixed during a long time. First, the PEM was rotated to a position where the SHS disappeared, i.e., φ_L was set to zero. Next, a relatively strong magnetic field was applied in order to increase the gliding angle to its prescribed value, φ_f (in most cases to 16 $^{\circ}$). As soon as the gliding angle attained this value, the magnetic field was varied in a way that the gliding angle should remain constant. In Fig. 1, the gliding angle, the magnetic field and the twist deformation, θ_L , is shown as a function of time. As it can be seen from the figure, the gliding angle stabilized in around 200 s. After stabilization both the magnetic field and the twist deformation decreased monotonically.

In Fig. 2, we show $\theta_L - \theta_0$, inferred from the first harmonic signal, on a logarithmic scale for different temperatures. After stabilization of the gliding angle a linear relation is obtained, i.e.,

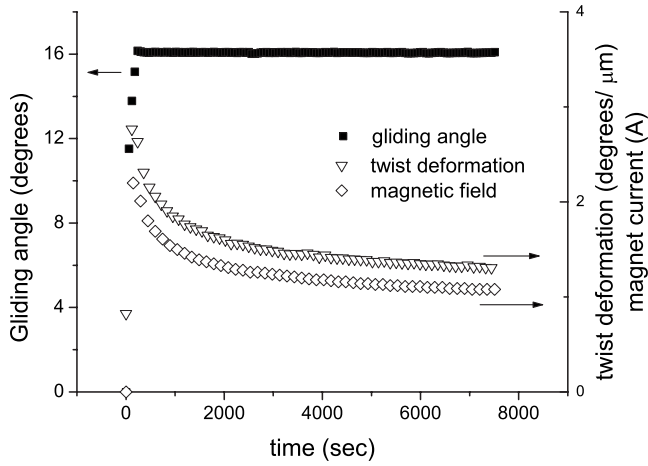


FIG. 1. The gliding angle (φ_L), the twist deformation at the polymer-nematic interface (θ_L) and the magnetic field strength as a function of time. The magnetic field is characterized by the current passed through the electromagnet, 1 A \approx 0.1 tesla. Temperature 30 °C.

$$\theta_L - \theta_0 = At^{-\beta} \quad (3)$$

with $\beta \approx 0.39$, independently from the temperature [12]. The factor A , however, shows a strong temperature dependence; the gliding process speeds up as the temperature is increased, as expected.

B. Short-term measurements

To investigate the early period of the gliding process, the magnetic field was applied for a short time (order of seconds). The first and second harmonic signals were displayed on an oscilloscope. From the data the time dependence of φ_L and $\theta_L - \theta_0$ could be obtained. An example of the measured curves is given in Fig. 3(a).

In Fig. 3(b), we plot φ_L against $\theta_L - \theta_0$ for different times of application of the magnetic field. As it can be seen, the curves deviate considerably from linear; moreover signifi-

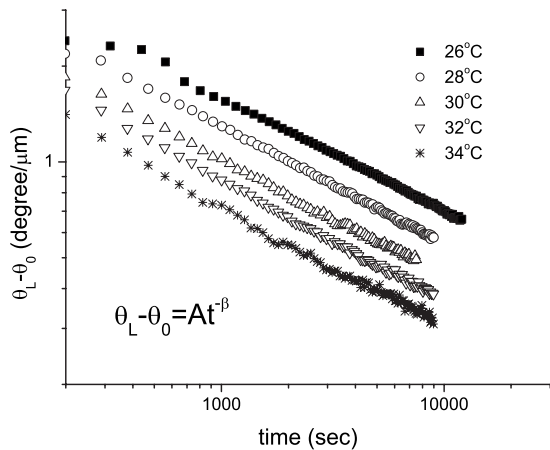
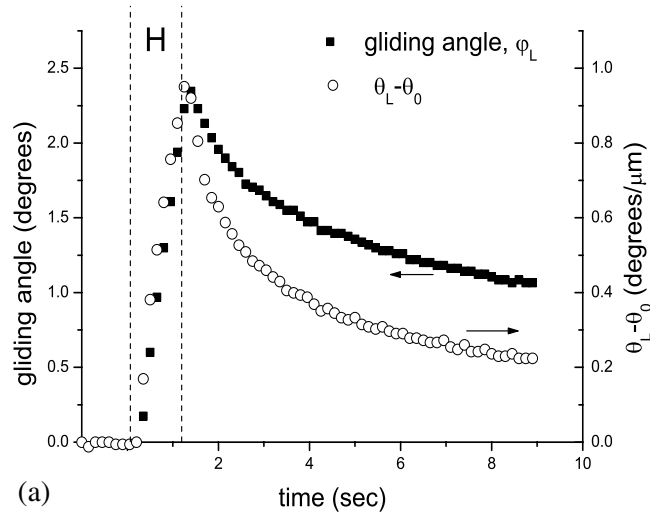
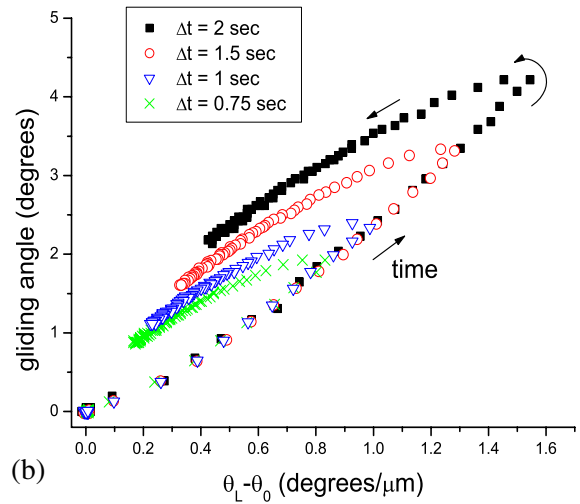


FIG. 2. The twist deformation at the surface with respect to its equilibrium value as a function of time, on a log-log scale, at different temperatures. For all curves $\beta \approx 0.38$.



(a)



(b)

FIG. 3. (Color online) (a) $\theta_L - \theta_0$ and the gliding angle as a function of time. The magnetic field was applied in the 0–1 s interval, its strength was 1 A. (b) The gliding angle as a function of $\theta_L - \theta_0$ for different application times of the magnetic field. Temperature 30 °C.

cant hysteresis was observed for up and down variation of the gliding angle, even with the shortest application period (0.75 s). As pointed out in the Introduction, this fact indicates that the easy axis or/and the anchoring strength must have changed during the application of the magnetic field, i.e., gliding occurred. The gliding is important even on a time scale below a second.

IV. INTERPRETATION

In the experiments it is possible to measure two quantities, the director and the twist deformation, both at the PEMA surface. These two quantities are interrelated by the balance of surface torques, which requires (in a linear approximation),

$$\xi\theta_L = -(\varphi_L - \varphi_e), \quad (4)$$

where ξ is the extrapolation length and φ_e is the azimuthal angle of the easy axis. The balance is established in microseconds for strong anchoring and in milliseconds for weak one [2], so from the point of view of the present experiments it can be considered to hold instantaneously. The two parameters, ξ and φ_e cannot be separated from the data. As two extreme cases we can suppose; (i) the anchoring strength is constant and the drift of the easy axis causes the gliding; (ii) the easy axis is unchanged during the field-induced process and the anchoring strength is changing in a such a way to cause the observed gliding. To interpret the data, a model of the interface properties is necessary.

In the model, first proposed in [8], it is assumed that the polymer chains at the interface possess a certain degree of orientational order. The alignment of the chains can be characterized by a two-dimensional order parameter tensor, \mathbf{Q} . The anisotropic part of the interfacial energy per unit area is $\frac{1}{4}W_a\mathbf{n}_s\mathbf{Q}\mathbf{n}_s$, where $\mathbf{n}_s = \{\cos \varphi_L, \sin \varphi_L\}$ is the director at the surface and W_a is a constant, characterizing the interaction energy between the liquid crystal molecules and the polymer chain segments. According to the idea, put forward in [8], the orientational order of the chains at the interface is due to the influence of the anisotropic liquid crystal potential and the order parameter tensor can change if the surface alignment of the liquid crystal is changed. Keeping φ_L fixed, after a long time the order parameter tensor reaches an equilibrium value, which can be written as

$$\mathbf{Q}_{eq} = Q_0 \begin{pmatrix} \cos 2\varphi_L & \sin 2\varphi_L \\ \sin 2\varphi_L & -\cos 2\varphi_L \end{pmatrix}. \quad (5)$$

Q_0 is the equilibrium value of the scalar order parameter.

In the model the dynamics of \mathbf{Q} is characterized by a distribution of relaxation times [8]. We assume that different segments of the polymer chains relax with different relaxation times toward the same equilibrium. The fraction of chain segments, which relax with a time constant between τ and $\tau+d\tau$ is $g(\tau)d\tau$ and their order parameter tensor is denoted by $\mathbf{q}(\tau)$. The rate equation is therefore

$$\frac{d\mathbf{q}(\tau)}{dt} = -\frac{\mathbf{q}(\tau) - \mathbf{Q}_{eq}}{\tau} \quad (6)$$

and

$$\mathbf{Q} = \int_0^\infty g(\tau)\mathbf{q}(\tau)d\tau. \quad (7)$$

The surface director is determined by the balance of surface torques [8],

$$\theta_L - \theta_0 = \frac{\xi_0}{2Q_0}(Q_{xx} \sin 2\varphi_L - Q_{xy} \cos 2\varphi_L), \quad (8)$$

where $\xi_0 = K_2/(W_a Q_0)$ is the extrapolation length for the equilibrium order parameter tensor [13].

In order to analyze the first type of experiment, we neglect the initial period, in which the gliding angle is stabilized to the prescribed fixed value, i.e., we assume

$$\varphi_L = \begin{cases} 0 & t \leq 0 \\ \varphi_f & t > 0 \end{cases}. \quad (9)$$

This approach can be used for $\varphi_f < 45^\circ$ and it is suitable to describe the asymptotic behavior of gliding. The initial condition for the order parameter tensors is $\mathbf{q}(\tau)|_{t=0} = Q_0\mathbf{1}$, where $\mathbf{1}$ denotes the unit tensor. For $t > 0$

$$Q_{eq,xx} = Q_0 \cos 2\varphi_s, \quad Q_{eq,xy} = Q_0 \sin 2\varphi_s. \quad (10)$$

Combining Eqs. (6)–(8) and (10), we get

$$\theta_L - \theta_0 = -\frac{\sin 2\varphi_s}{2\xi_0} I(t) \quad \text{with} \quad I(t) = \int_0^\infty e^{-t/\tau} g(\tau) d\tau. \quad (11)$$

From the fact that on logarithmic scale $\theta_L - \theta_0$ is linear with respect to t (see Fig. 2) we conclude that $g(\tau)$ follows a power law with an exponent of $1 + \beta$ —at least at large τ s. For simplicity we assume that there is a cutoff time, τ_0 , below which $g(\tau) = 0$,

$$g(\tau) = \begin{cases} C\tau^{-(1+\beta)} & \tau > \tau_0 \\ 0 & \tau \leq \tau_0 \end{cases}, \quad (12)$$

where $C = \tau_0^\beta / \beta$ is a normalizing constant. With this form of $g(\tau)$

$$I(t) = \frac{1}{\beta} \int_{\tau_0}^\infty e^{-t/\tau} \frac{\tau_0^\beta}{\tau^{1+\beta}} d\tau. \quad (13)$$

The asymptotic behavior of the above expression is [14] $I(t) \rightarrow \Gamma(\beta) / \beta (\tau_0/t)^\beta$ for $t \gg \tau_0$, where Γ denotes the gamma function. Therefore,

$$\theta_L - \theta_0 \rightarrow \sin 2\varphi_s \frac{\Gamma(\beta)}{2\beta\xi_0} \left(\frac{\tau_0}{t}\right)^\beta, \quad (14)$$

in accordance with the experimental observations.

From the experimental data it is only possible to determine the value of τ_0^β / ξ_0 , but not separately the cutoff time and the extrapolation length. This fact was already noted in [8].

To interpret the short-time experiments, where only small gliding takes place, we can linearize Eqs. (5) and (8) with respect to the gliding angle, φ_L . The linearization leads to the following set of equations,

$$\varphi_L = \xi_0(\theta_L - \theta_0) + \psi_0,$$

$$\psi_0 = \int g(\tau)\psi(\tau)d\tau,$$

$$\frac{d\psi(\tau)}{dt} = -\frac{\psi(\tau) - \varphi_L}{\tau}. \quad (15)$$

Here ψ_0 denotes the azimuthal angle of the “easy axis” of the polymer layer, i.e., the direction of the eigenvector of the order parameter tensor; $\psi(\tau)$ is the azimuthal angle of the easy axis of the chain segments with relaxation time τ , i.e., the direction of the eigenvector of the tensor $\mathbf{q}(\tau)$. The initial condition is $\psi(\tau)|_{t=0} = 0$.

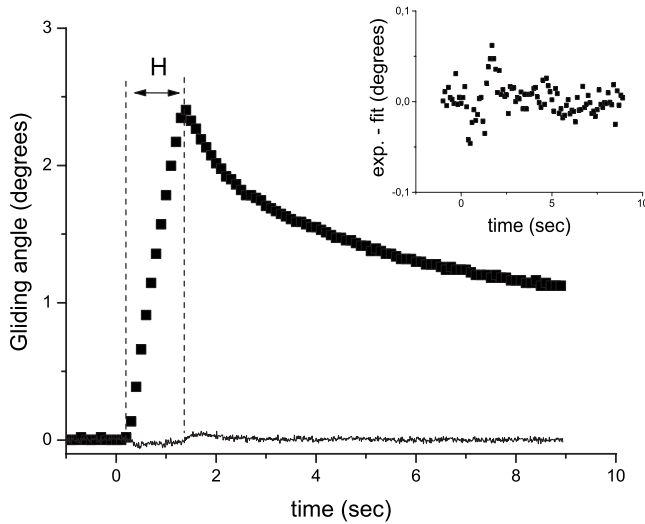


FIG. 4. Squares: the calculated gliding angle for the curve plotted in Fig. 3, with $\tau_0^* = 0.05$ s, $\xi_0 = 20.1$ nm and $\beta^* = 0.185$. Continuous line and inset: deviation between the theoretical and experimental curves.

In order to compare the theoretical description with the experimental one, we calculated φ_L as a function of time according to Eq. (15), taking the θ_L values from the measured first harmonic signal. The extrapolation length [which plays the role of a scaling factor for φ_L in Eq. (15)] was chosen so that the peak value of φ_L should coincide in the experimental and fitted curves. First we tried to fit the experimental data with a single relaxation time {we note that this is equivalent with introducing a surface viscosity term in Eq. (4) [2]}. No satisfactory agreement was obtained with any choice of τ . Assuming, however, a similar power law for $g(\tau)$ as in the long term case [see Eq. (12)], an excellent agreement could be achieved between theory and experiment. An example is shown in Fig. 4. The parameters of the power-law distribution, however, were not the same as in the case of the long-term behavior. The exponent (which we now denote by β^*) was found to be 0.185, i.e., approximately one half of the value observed in the long term experiments. Furthermore, we found a good fit only if we chose the cutoff time, τ_0^* , to be smaller than a certain value. In Fig. 5, we demonstrate the agreement on the example of a curve obtained at 30 °C, with the application of the magnetic field for 1 s. The standard deviation between the experimental and theoretical curves is presented as a function of τ_0^* , assuming $\beta^* = 0.185$ and adjusting the extrapolation length in the way described above. As it can be seen from the figure, the standard deviation is very small for $\tau_0^* \leq 0.02$ s and starts to increase as τ_0^* is chosen to be larger than 0.1 s. From this fact we conclude that the actual value of τ_0^* is lower than 0.1 s, so gliding occurs on very short time scales too. The corresponding extrapolation length is smaller than 20 nm, therefore, according to the present model, the azimuthal anchoring is very strong.

We note that from the short-term measurements it is again not possible to determine independently the two parameters, ξ_0 and τ_0^* , only to give an upper limit for their values. In the Appendix, we show that for the specific form of the distri-

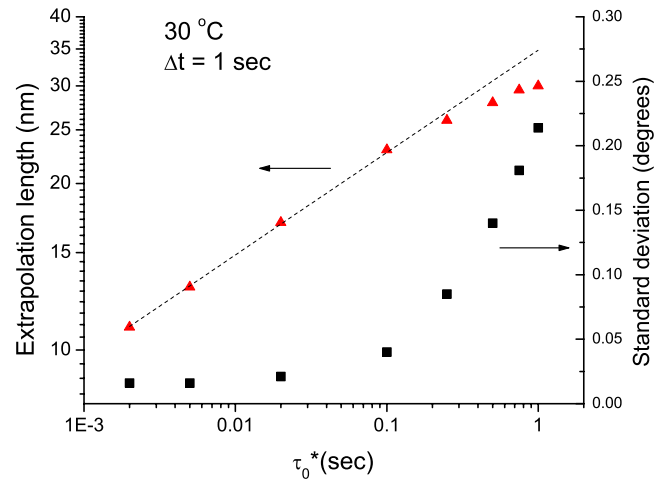


FIG. 5. (Color online) The standard deviation between the calculated and measured curves (squares) and the adjusted extrapolation length (triangles) as a function of τ_0^* . The dashed line indicates the relation $(\tau_0^*)^{\beta^*} / \xi_0 = \text{const}$.

bution function, given in Eq. (12), it is only possible to deduce $(\tau_0^*)^{\beta^*} / \xi_0$ from the measurements, just as in the case of long-term experiments. The argument presented in the Appendix, however, is not restricted to the specific form of $g(\tau)$. The components of the polymer with sufficiently short relaxation times can be considered either to speed up gliding or, equivalently, to reduce the elastic anchoring energy. From the macroscopic experiments it is not possible to separate gliding on a short time scale (in our experiments below 0.1 s) from the elastic anchoring. This fact also means that the cut-off character of $g(\tau)$ is not crucial for our model. We can infer from the experiments that the power-law distribution holds down to a time approximately 0.1 s, but no information is contained in them about the distribution function below that time.

An analysis of the model shows that in both of the two limiting cases discussed above (the long-term asymptotic behavior and the very early stage of gliding), the rotation of the surface director is connected first of all with the drift of the easy axis, while the anchoring energy is almost constant (case a; at the beginning of this Section). However, during the whole gliding process, the model predicts a temporal decrease of the anchoring energy.

Finally we compare the distribution functions obtained from the long-term and the short-term measurements. When the long-term behavior of gliding is calculated using the short-term distribution function, the experimentally observed $\theta_L - \theta_0$ values for large times are significantly overestimated. A possible reason for this circumstance is that different types of conformational transitions are responsible for the short-term and long-term gliding. The fact that the exponent of the long-term distribution function is about twice of that of the short-term one might indicate that a two-step conformational transition is responsible for the long-term behavior of gliding. While the transitions associated with the short-term gliding may involve a single energy-barrier crossing, those transitions, which causes the long-term gliding could consist of two subsequent barrier crossings.

V. SUMMARY

We found that director gliding on PEMA layers is a very dispersive process that starts below a fraction of a second and lasts at least for several hours. We characterized the process by a distribution of relaxation times. A power-law distribution of the relaxation times is in excellent agreement with experimental results both for long-time and short-time gliding. From the short-time scale experiments we concluded that the azimuthal anchoring of the nematic liquid crystal on PEMA layers is very strong. Although the precise value of the extrapolation length cannot be deduced from the experimental results, only an upper limit can be given for it, this upper limit is comparable with those found on rubbed or UV cross-linked polyimide layers [10,11]. We believe that these features are compatible with the picture suggested earlier, according to which gliding is connected with nematic-order-induced conformational transitions in the interfacial polymer chains.

APPENDIX

First, we show that for sufficiently small τ , the easy axis belonging to the appropriate chain segments, $\psi(\tau)$, coincides with the surface director.

The solution of the third equation in Eq. (15), obeying the initial conditions $\psi(\tau,0)=0$ and $\psi_L(0)=0$, can be written as

$$\psi(\tau,t) = \frac{1}{\tau} \int_0^t \varphi_L(t') e^{-(t-t')/\tau} dt'. \quad (\text{A1})$$

After some mathematical manipulation, one obtains

$$\psi(\tau,t) = \varphi_L(t) - \tau \frac{d\psi_L}{dt}, \quad (\text{A2})$$

where

$$\frac{d\psi_L}{dt} = \frac{\int_0^t d\varphi_L/dt e^{-(t-t')/\tau} dt'}{\int_0^t e^{-(t-t')/\tau} dt'}$$

is a weighted average of the time derivative of the gliding angle in the $[0,t]$ interval. For large τ s the weighted average is around the mean value of the time derivative in the interval; for small τ s it is approximately equal to the time derivative at the time t . If τ is small enough that $\tau d\psi/dt$ can be neglected, the relation $\psi(\tau,t) \approx \varphi_L(t)$ holds.

Let us now assume a distribution of the relaxation times $g(\tau)=g_1(\tau)$ with $\tau_0^*=\tau_1$ and $\xi=\xi_1$. Next, let us consider a relaxation time $\tau_2 > \tau_1$. We suppose that τ_1 and τ_2 are both so short times that the easy axis belonging to the chain segments with relaxation times $\tau_1 > \tau > \tau_2$ follow instantaneously the surface director, i.e.,

$$\psi(\tau) \approx \varphi_L \quad \text{for} \quad \tau_1 > \tau > \tau_2. \quad (\text{A3})$$

Using this approximation, we can rewrite Eq. (15) as

$$\varphi_L = \xi_1(\theta_L - \theta_0) + \varphi_L \int_{\tau_1}^{\tau_2} g_1(\tau) d\tau + \int_{\tau_2}^{\infty} g_1(\tau) \psi(\tau) d\tau, \quad (\text{A4})$$

which can be written in the form

$$\varphi_L = \xi_2(\theta_L - \theta_0) + \hat{\psi}_0, \quad (\text{A5})$$

$$\hat{\psi}_0 = \int_{\tau_2}^{\infty} g_2(\tau) \psi(\tau) d\tau,$$

with $\xi_2 = \xi_1 / (1 - \int_{\tau_1}^{\tau_2} g_1(\tau) d\tau)$ and $g_2(\tau) = g_1(\tau) / (1 - \int_{\tau_1}^{\tau_2} g_1(\tau) d\tau)$. Note that $g_2(\tau)$ corresponds to a power-law distribution with $\tau_0^* = \tau_2$. That means that replacing τ_1 and ξ_1 by τ_2 and ξ_2 the same fit is obtained for φ_L , provided that τ_2 is short enough to obey the approximation Eq. (A3). Inserting the power-law distribution into the expression for ξ_2 one obtains $\tau_2^{\beta} / \xi_2 = \tau_1^{\beta} / \xi_1$. As a consequence, it is only possible to deduce $(\tau_0^*)^{\beta} / \xi_0$ from the measurements, just as in the case of long-term experiments.

-
- [1] E.g., S. Faetti, in *Physics of Liquid Crystalline Materials*, edited by I. C. Khoo and F. Simoni (Gordon and Breach, Philadelphia, 1991), Chap. 12.
- [2] G. E. Durand and E. G. Virga, *Phys. Rev. E* **59**, 4137 (1999).
- [3] P. Vetter, Y. Ohmura, and T. Uchida, *Jpn. J. Appl. Phys.* **32**, L1239 (1993).
- [4] V. P. Vorflusev, H.-S. Kitzerow, and V. G. Chigrinov, *Appl. Phys. Lett.* **70**, 3359 (1997).
- [5] S. Faetti, M. Nobili, and I. Raggi, *Eur. Phys. J. B* **11**, 445 (1999).
- [6] Yu. Kurioz, V. Resetnyak, and Yu. Reznikov, *Mol. Cryst. Liq. Cryst.* **375**, 535 (2002).
- [7] S. Joly, K. Antonova, Ph. Martinot-Lagarde, and I. Dozov, *Phys. Rev. E* **70**, 050701(R) (2004).
- [8] I. Jánossy and T. I. Kósa, *Phys. Rev. E* **70**, 052701 (2004).
- [9] A. Romanenko, V. Reshetnyak, I. Pinkevich, I. Dozov, and S. Faetti, *Mol. Cryst. Liq. Cryst.* **439**, 1867 (2005).
- [10] I. Jánossy, *J. Appl. Phys.* **98**, 043523 (2005).
- [11] S. Faetti, K. Sakamoto, and K. Usami, *Phys. Rev. E* **75**, 051704 (2007).
- [12] In [8], where a similar cell was used, a smaller β value was found. The reason maybe that in the present experiments the final measurements were performed several month after the sample preparation, which gave enough time for the stabilization of the equilibrium state of the polymer-nematic interface.
- [13] The definition of ξ given here differs in the factor Q_0 from that in [8]. The present definition corresponds to the usual description of the extrapolation length.
- [14] E. Janke, F. Emde, and F. Lösch, *Tables of Higher Functions*, 6th ed. (McGraw-Hill, New York, 1960).